Quantitative study of the hardness property of laser surface alloyed aluminium AA1200

by A.P.I. Popoola*, S.L. Pityana*†, T. Fedotova*, and O.M. Popoola*

Transaction Paper

Synopsis

Aluminium AA1200 was laser alloyed with a combination of nickel and titanium diboride using different weight ratios. Chemical reactions took place with the formation of different phases. The characterization of the alloyed surfaces was carried out by x-ray diffraction (XRD), optical and scanning electron microscopes. The alloyed surfaces are composed of the initial phase of Al-Ni dendrites and eutectics of TiB_2/Al and TiB_2/Ni distributed on the initial phase. Experimental results obtained showed that Al-Ni intermetallics brought about a significant increase in the hardness property of Al; however, these intermetallics are highly brittle and prone to fail by brittle fracture or stress corrosion cracking when put in service. The addition of TiB_2 brought about a reduction in the formation of these intermetallic phases. A microhardness increase of over 10 times the hardness of the substrate was achieved.

Keywords
Dendrites, intermetallics, metal composite, Nd: YAG laser.

Introduction

Mechanical and chemical properties of metals and their alloys can be enhanced by the application of surface coatings. Today, different surface treatments are in use but among them laser surface alloying (LSA) is a well known process[1,3]. LSA is widely used for fabricating various laser coatings on the surfaces of metals and their alloys; these laser coatings are characterized by relatively high hardness, better wear, abrasive, corrosion and erosion resistances. The improved mechanical and chemical properties displayed by these coatings is largely due to the numerous advantages associated with this method. Examples are: high energy density, refined microstructure in the alloyed zone due to high cooling/solidification rates that minimize its effect on the substrate; the bulk of the substrate acts as a heat sink and it is left unaffected[2,3].

Aluminium is the third most abundant element after oxygen and silicon, apart from its mineral being abundant on the earth crust; aluminium is also relatively cheap compared to other metals. It is a metal that is easily fabricated, the automobile industries utilize aluminium and its alloys mainly because of their light weight. However, aluminium and its alloys exhibit low hardness, that is, inadequate resistance to plastic deformation. Consequently, they have poor tribological properties, hence potential applications of Al-alloys are limited[2].

Aluminium alloy hard particle composite/intermetallics can be synthesized by laser alloying process through reinforcement of hard particles. Improved properties can be achieved by the use of lasers as long as the laser processing parameters are carefully chosen. LSA is usually carried out by impinging the laser energy on the surface of the substrate and simultaneously depositing the reinforcement powder into the melt pool. The powder used for reinforcement is selected according to engineering property requirements, e.g. hardness, corrosion protection, wear and fatigue protection. The result of LSA is a substrate surface with improved properties performance[2].

Hardness is a property that has been studied by different researchers: Wang *et al.* deposited a TiC/Ni-based alloy composite coating on to the surface of AISI 4140 chromium molybdenum steel. Microhardness measurements were taken of 50 per cent TiC composite coating and 50 per cent TiC/Ni-based alloy with La_2O_3 composite coating. The result showed that the addition of La_2O_3 can significantly increase the microhardness of the clad coating[1]. Majumdar *et al.* developed *in situ* titanium boride dispersed Al based metal matrix composite layer onto the surface of Al substrate to improve its wear resistance property. The authors found that the volume fraction of particles decreases with increases in

* *Tshwane University of Technology, Pretoria, South Africa.*

† *Center for Scientific and Industrial Research—National Laser Centre, Pretoria, South Africa.*

 SA ISSN 0038–223X/3.00 + 0.00. Paper received Dec. 2010; revised paper received Mar. 2011.

applied laser power. Increasing scan speed increases the area fraction of particle which resulted because of lower depth of melting at a higher scan speed (due to interaction time) and decreased dilution. The average microhardness of the composite layer was found to vary with process parameters[2]. Vaziri *et al.* studied the laser surface alloying of aluminium with nickel. The authors found that laser alloying led to a significant hardening effect. The hardness of the alloyed layer was 10–15 times the value for base Al[3]. Chen and Wang fabricated TiC reinforced nickel aluminides composite coating on electrolyzed nickel plate by laser cladding using Ni-Al-Ti-C alloy powders. From the result of the investigation, it was found that the coating had a high and uniform hardness distribution because of the rapidly solidified fine microstructure and the presence of very high hardness of TiC reinforcing phased[4].

In this work, a combination of powders (TiB_2 and Ni) is chosen to obtain alloys of good properties. As reinforcement material, TiB_2 is chosen due to its high hardness, low density, good oxidation resistance and thermodynamic stability in aluminium; therefore TiB_2 containing metal matrix composites possess outstanding mechanical properties, corrosion resistance and relatively good ductility. Very hard intermetallic phases with high strength are formed between nickel and some alloying elements[4]. It has been reported that Ni powder gave significant improvement in the hardness of Al, even up to 1000 HV. However, the intermetallics formed by Al-Ni are known to be very brittle compounds and are therefore prone to fail by brittle fracture or stress corrosion cracking when put in service. This work seeks to fabricate laser coatings on Al that will be reasonably hard and yet not excessively brittle. It is hoped that the synthesis of Ni and TiB_2 would produce an intermetallic matrix composite coating on Al substrate that will combine the high hardness of Al-Ni intermetallics with the ductility of TiB_2 contained metal matrix composite (MMC) to produce a new alloy of intermediate hardness with good surface quality.

The current investigation presents quantitative study of the hardness properties of different laser coatings. The influence of reinforcement proportion (Ni and TiB_2 combined in different weight ratios) on the hardness properties, the microstructures and phases of the resultant alloys are studied.

Experimental

Aluminium AA1200 is a commercially pure metal. The substrate was cut and machined to dimensions 100 x 100 x 6 mm. It was then prepared for laser surface alloying by sandblasting to clean the surface and improve the metal's absorptivity of the laser beam.

The two alloying powders used for this work are: nickel (Ni) and titanium diboride (TiB_2). These powders were mixed in different weight ratios as 30 wt. per cent TiB_2 + 70 wt. per cent Ni; 40 wt. per cent TiB_2 + 60 wt. per cent Ni; 50 wt. per cent TiB_2 + 50 wt. per cent Ni; and for comparison, laser surface alloying of only Ni (100 per cent Ni) and only TiB_2 (100 per cent TiB_2) was also performed. The powder particle morphology and size distribution were analysed using a scanning electron microscope SEM and Malvern Mastersizer 2000 image analyser. A Philips PW 1713 X-ray diffractometer fitted with a monochromatic Cu Kα radiation set at 40 kV and 20 mA was used to determine the phase composition of powder. The scan was taken between 10° and 80° two theta with a step size of 0.02 degree. Phase identification was done using Philips Analytical X'Pert HighScore® software with an in-built International Centre for Diffraction Data (ICSD) database.

A Rofin Sinar Nd:YAG solid-state laser was used for laser surface alloying; it consists of an off-axes nozzle which is used for powder feeding. The laser is delivered to the target material through fibre optics. A Kuka robot is used to move the alloying head. The shielding gas used was argon to shroud the molten pool from the atmosphere to prevent oxidation during the alloying process. Table I shows the laser processing parameters used and the composition of powder mixture. The laser scanning speeds were varied in a series of tests in order to get the optimum laser processing parameters.

Metallographic preparation

The cross-section of samples were cut and mounted. Samples were ground from 80 to 1200 grit on SiC paper. The samples were then polished using diamond impregnated clothes of 3 μm down to 1 μm followed by an oxide polishing (OP-S) system. In the OP-S system, polishing is achieved through a combination of chemical treatment (the solution has a pH of 8) and gentle abrasive action, this allows selective polishing

Table I

Laser processing parameters and composition used during the laser alloying experiments

Sample no.	System (Al- TiB_2-Ni) composition	Power (kW)	Beam diameter (mm)	Scan speed (m/min)	Powder feed rate (g/min)	Shielding gas	Shielding gas flow (ℓ/min)
17	30%TiB_2 + 70%Ni	4	3	0.6	2	Argon	4
18	30%TiB_2 + 70%Ni	4	3	0.8	2	Argon	4
19	30%TiB_2 + 70%Ni	4	3	1.0	2	Argon	4
20	30%TiB_2 + 70%Ni	4	3	1.2	2	Argon	4
23	50%TiB_2 + 50%Ni	4	3	0.6	2	Argon	4
24	50%TiB_2 + 50%Ni	4	3	0.8	2	Argon	4
25	50%TiB_2 + 50%Ni	4	3	1.0	2	Argon	4
26	50%TiB_2 + 50%Ni	4	3	1.2	2	Argon	4
27	40%TiB_2 + 60%Ni	4	3	0.6	2	Argon	4
28	40%TiB_2 + 60%Ni	4	3	0.8	2	Argon	4
29	40%TiB_2 + 60%Ni	4	3	1.0	2	Argon	4
30	40%TiB_2 + 60%Ni	4	3	1.2	2	Argon	4

of the softer phases. The microstructures of the new phases were characterized by optical and scanning electron microscopes. The characteristics of the phases were studied by means of x-ray diffraction.

Microhardness test

The microhardness measurement of the samples was performed along the depth in the direction of the coating using a Matsuzawa Vickers microhardness tester with an applied load of 100 g and spacing of 100 μm for 15 seconds. Average microhardness was taken from the results of five indents values for all samples in order to get a good representation of the overall microhardness.

Results and discussion

Characterization of starting materials

Particle size analysis of powders

Table II is the summary of the particle sizes of the starting powders.

The results from the Table II show that nickel has the highest average particle size, while the 50:50 powder mixtures of TiB_2 and Ni has the lowest average particle size. It was also observed that only the nickel powder showed average particle size greater than 30 μm.

Phase analysis of reinforcement powders

Typical XRD spectrum of the mixtures can be seen from Figure 1. The XRD patterns of the powder mixtures (Ni and TiB_2) showed some similarities; however, there were differences in their peaks. The similarities in their patterns confirmed the presence of both Ni and TiB_2; the differences in their peaks could be as a result of the different weight percentages in which they were mixed. It was also observed that the intensity of the powders increased as the percentage of TiB_2 in the mixtures increased.

The chemical composition of the substrate is shown in Table III. The X-ray spectrum of AA1200 can be seen in Figure 2. This shows the identified phases present in the substrate; only aluminium peaks can be seen, substrate is pure. The microhardness value of the AA1200 is 24.0 ± 0.4 $HV_{0.1}$.

Microstructural study of powder

The micrographs obtained from the SEM analysis of the powders are shown in Figures 3a and 3b. SEM image of the nickel powder shown in Figure 3a reveals the ball-like shape of the powder, the SEM micrograph of the TiB_2 powder in Figure 3b reveals the morphology of the TiB_2 powder to be irregular in shape and clustered together. Figure 4 shows the SEM/EDS of a typical powder mixture; the presence of both additions, the nickel powder evenly distributed within the TiB_2 matrix can be seen clearly. All starting materials have been proven to be pure.

Characterization of laser coatings

Microstructure and composition of the laser coatings

Figure 5 is a stereo micrograph of a laser coating which shows the heat affected and alloyed zones. The laser beam

Table II

Summary of the particle size of the starting powders

Powder	D_{10} (μm)	D_{50} (μm)	D_{90} (μm)
Ni	49.954	68.535	93.991
TiB_2	8.106	28.709	84.425
30%TiB_2+70%Ni	8.102	25.305	71.199
50%TiB_2+50%Ni	7.451	20.966	67.940
40%TiB_2+60%Ni	8.093	29.301	85.809

Table III

Chemical composition of the substrate material

Element	Al	Fe	Cu	Si
Composition (wt.%)	Balance	0.59	0.12	0.13

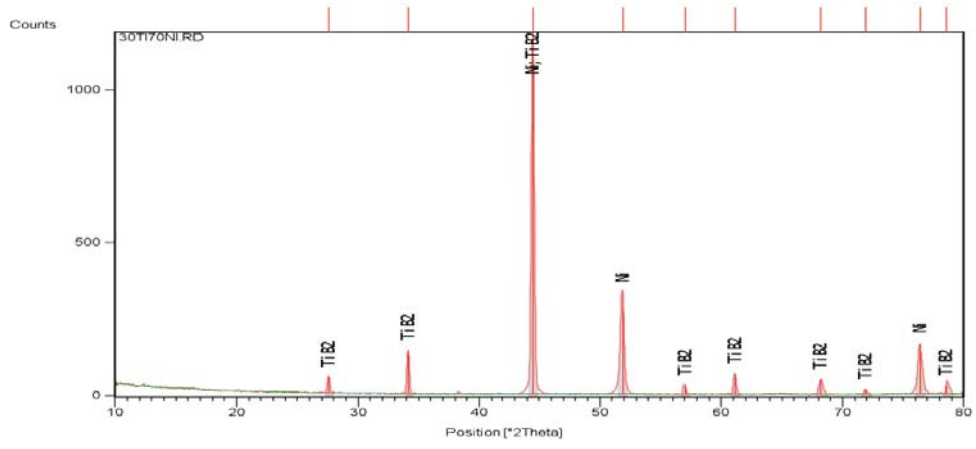

Figure 1—Typical X-ray spectrum of 30% TiB_2 + 70% Ni powder mixture

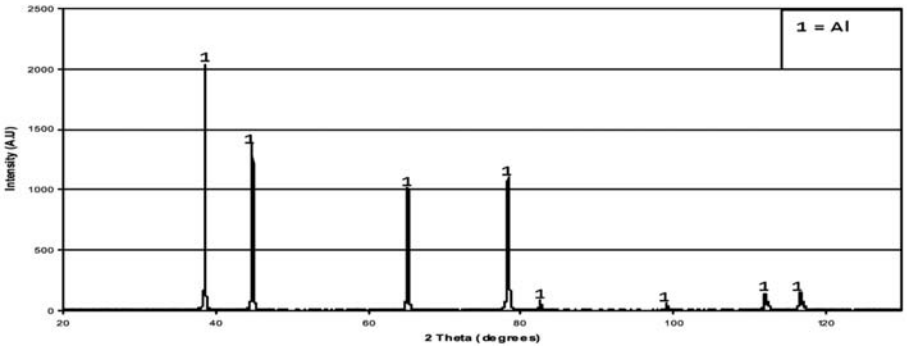

Figure 2—X-ray spectrum of AA 1200

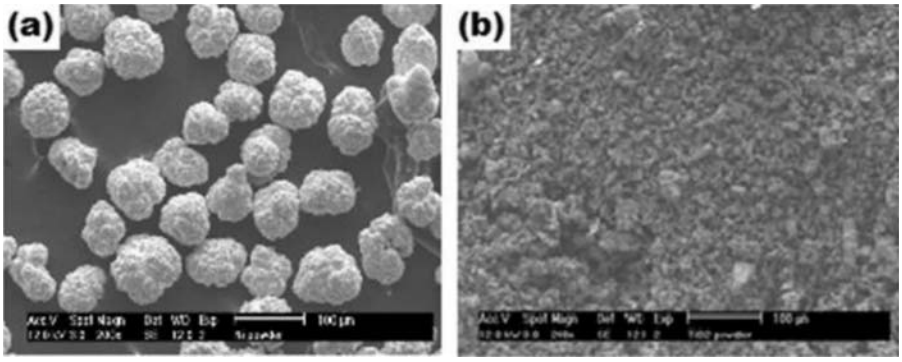

Figure 3—Scanning electron micrograph of (a) Ni powder and (b) TiB_2 powder

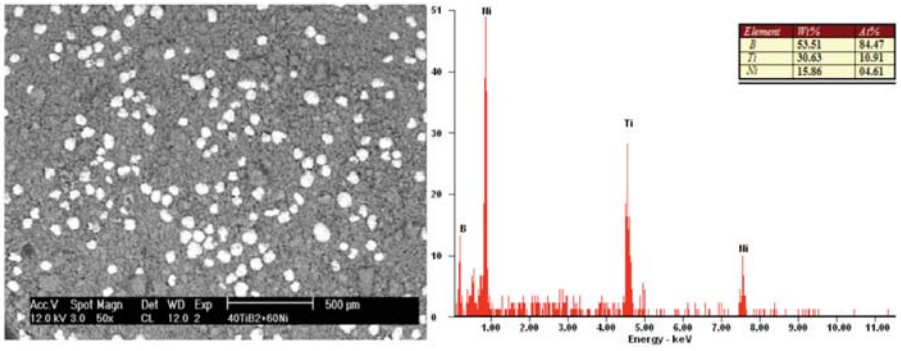

Figure 4—Typical scanning electron micrograph and EDS of 40% TiB_2 + 60% Ni

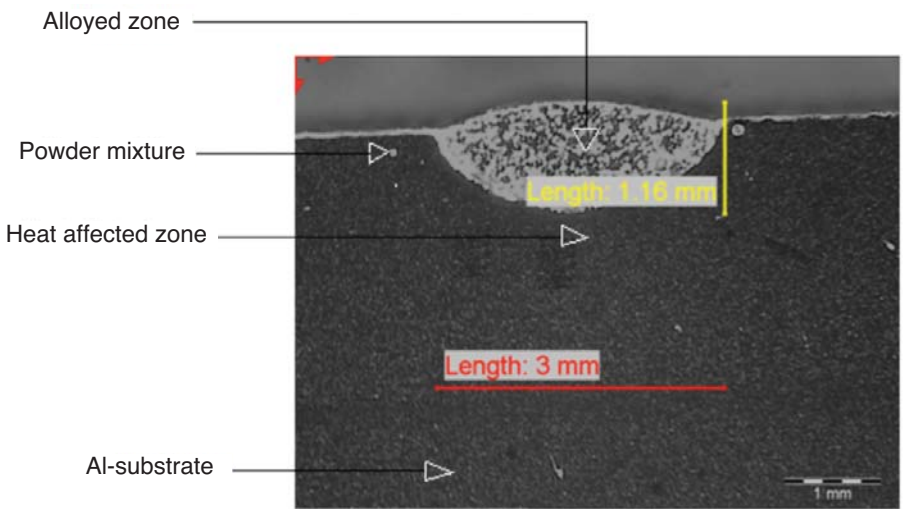

Figure 5—A typical micrograph of Al surface alloyed with combination of Ni and TiB_2 powder showing the alloyed and heat affected zones

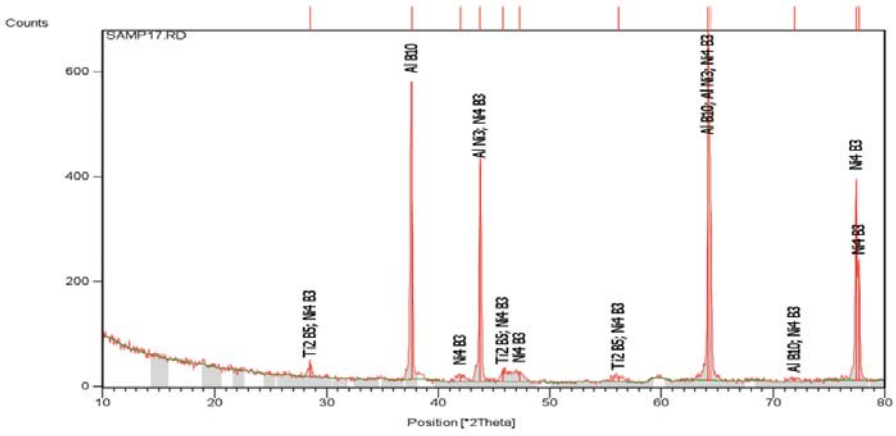

Figure 6—XRD spectrum of an aluminium surface alloyed 30% TiB_2 + 70% Ni (Sample 17)

impinges on the surface of substrate and its energy density led to the formation of a melt pool, the laser by means of a nozzle simultaneously injected the powder mixture into the melt pool.

Chemical reactions occurred that resulted into the formation of different compounds. However, it should be noted that the microstructure evolved depends largely on the laser processing parameters used. Aluminium composite so fabricated exhibits uniform dispersion of the particle in the matrix as well as good interface bonding between the ceramic phase and the metallic phase as shown in Figure 5. Laser coatings are crack free. The maximum depth of the coatings achieved was 1.44 mm for sample 17. The width of the laser track is approximately equal to that of the laser beam of 3 mm for all samples. The coatings were then characterized in terms of microstructure and phases.

30 wt. per cent TiB_2 + 70 wt. per cent Ni laser coatings

Figure 6 shows typical XRD spectrum for 30 wt. per cent TiB_2 + 70 wt. per cent Ni laser coatings. Three phases were identified in these micrographs which are the dendritic phase ($AlNi_3$), the Ni_4B_3 and TiB/TiB_2 phase (grey lumps).

Samples 17 and 20 have these three phases in common. $AlNi_3$ phase is an intermetallic phase that possesses dendritic structure and it is characterized by very high hardness. In the same way, the nickel borides are very hard compounds. Some of the phases, however, exhibited overlapping peaks. For all laser coatings regardless of powder proportion, the dendrites are composed of Al, Ni which is dispersed uniformly within the matrix of the substrate. However, the distribution of B and Ti are identical: they concentrate in the matrix and are characterized by poor dendrites formation. The EDS analysis of the samples confirmed the presence of Ni, Al, B and Ti elements. EDS analysis of selected areas indicated that the black regions are rich in Ti and the white regions are rich in Ni. From Figures 7a and 7b, the microstructures of samples 17 and 20 can be seen from the SEM micrographs. Figure 7a shows a very dense aluminium-nickel intermetallic dendritic phase to be dominant in the coating as a result of the high per centage of Ni (70 per cent) in the reinforcement.

50 wt. per cent TiB_2 + 50 wt. per cent Ni laser coatings

Figure 8 shows a typical XRD spectrum for 50 per cent TiB_2 + 50 per cent Ni laser coatings. The various phases identified in these coatings are Ni_4B_3, $TiO_{0.997}$, Ti, dendritic phase ($AlNi_3$) and TiB/TiB_2 phase (grey).

This set of coatings has similar phases identified in their spectrums as in the coatings prepared by 30 per cent TiB_2 + 70 per cent Ni except for $TiO_{0.997}$ phase. These coatings are dominated by $TiO_{0.997}$ in their microstructures. This can be attributed to the lower content of Ni and of course the

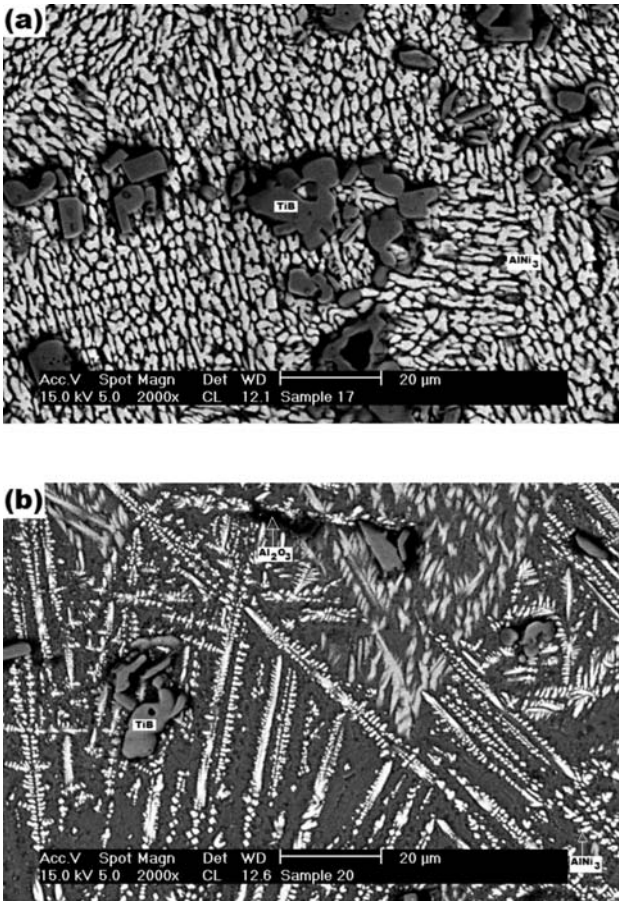

Figure 7—SEM micrographs of aluminium surface alloyed with 30% TiB_2 + 70% Ni (a) sample 17 and (b) sample 20. TiB_2, TiB phases (grey lumps); $AlNi_3$ white dendritic structure

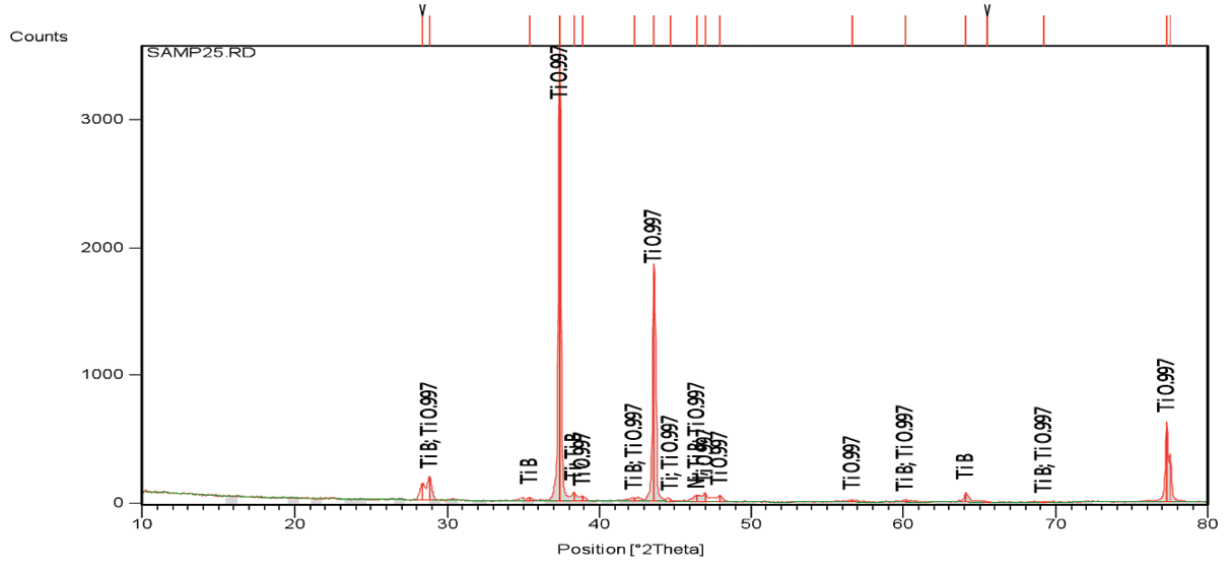

Figure 8—XRD spectrum of an aluminium surface alloyed 50% TiB_2 + 50% Ni (sample 25)

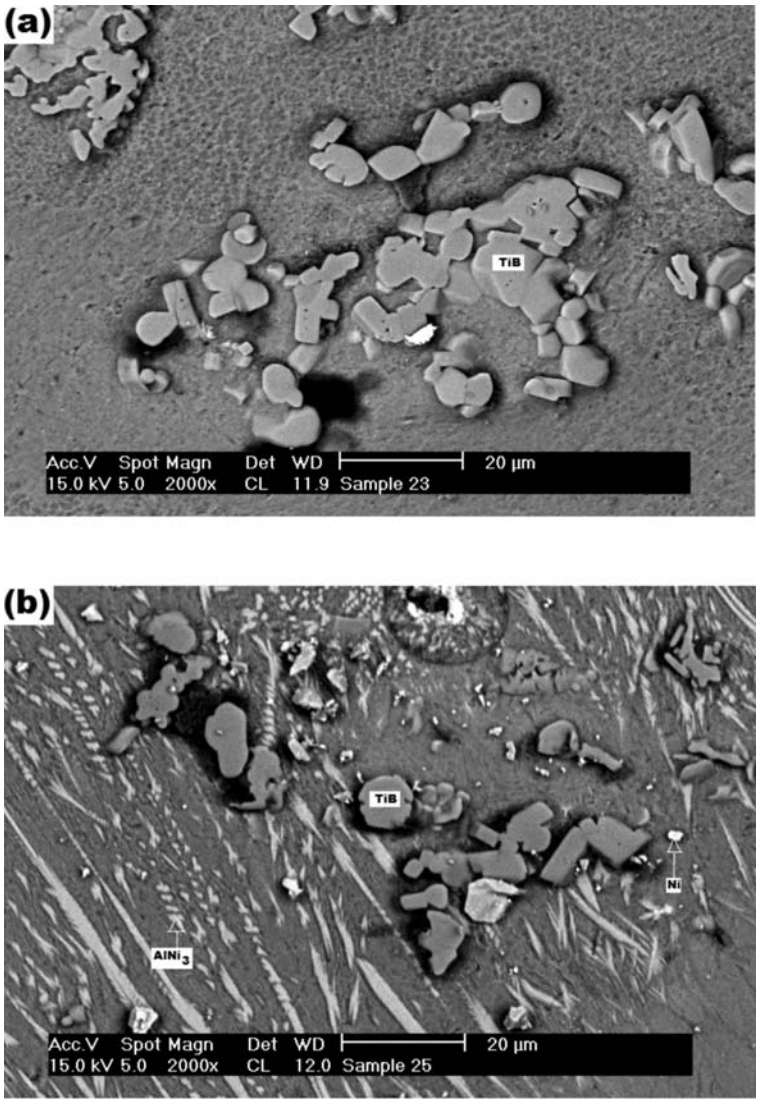

Figure 9—SEM micrographs of aluminium surface alloyed with 50% TiB_2 + 50% Ni (a) sample 25 and (b) sample 23 TiB_2. TiB phases (grey lumps); $AlNi_3$ white dendrite structure; Ni_4B_3, $TiO_{0.997}$

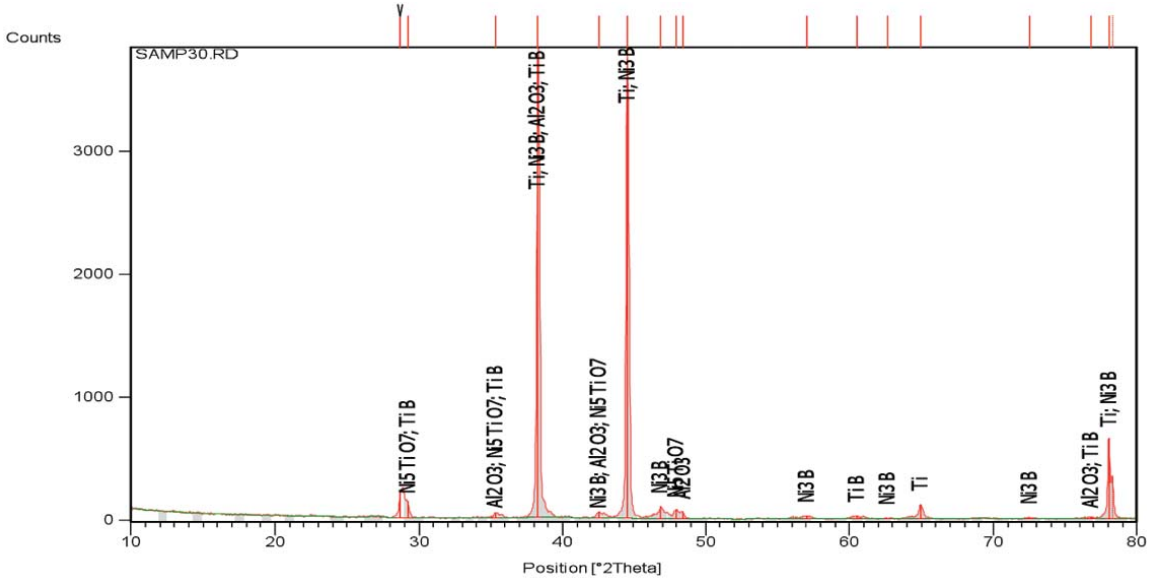

Figure 10—XRD spectrum of a typical aluminium surface alloyed 40% TiB_2 + 60% Ni (sample 30)

variations in scan speed. From Figures 9a and 9b, the microstructures of samples 23 and 25 can be seen from the SEM micrographs. Figure 9b is the SEM micrograph of sample 25. $TiO_{0.997}$ is the dominant phase exhibited by coating. The EDS analysis of the samples confirmed the presence of Ni, Al, B, Ti and O.

40 wt. per cent TiB_2 + 60 wt. per cent Ni laser coatings

Figure 10 shows a typical XRD spectrum for 40 per cent TiB_2 + 60 per cent Ni laser coatings. From the XRD pattern four phases were identified which are the dendritic phase $AlNi_3$, Ni_5TiO_7, Ni_3B, Al_2O_3.

The EDS analysis of the samples confirmed the presence of Ni, Al, B, O and Ti. Figures 11a and 11b show the microstructures of samples 29 and 30. Figure 11b is the SEM micrograph for sample 30 which is dominated by Al-Ni dendritic structure, Al_2O_3 and Ni_3B. Corundum is the second hardest natural mineral known to science. The hardness of corundum can be partially attributed to the strong and short oxygen-aluminum bonds. The high hardness of this sample can be explained by the presence of Al_2O_3.

In general, it can be concluded that the laser coatings are composed of the initial phase of Al-Ni dendrites and eutectics of TiB_2/Al and TiB_2/Ni distribution on the initial phase. The variation in the composition of the resultant phases was due to the influence of the reinforcement proportion and the scan speed. Since the parameter is a thermodynamic function of the input energy that affects the dependent process variables such as the interaction time and cooling rate; these are metallurgical parameters that determines the grain sizes and microstructures evolved.

Hardness results

With the Vickers hardness tester, the microhardness/depth profile for all samples tested was plotted. Table IV shows the properties of the alloyed layers. A good increase in the microhardness value was observed in the alloyed layers. The average microhardness for all samples was calculated by taking a minimum of 5 representative indent values from the results obtained.

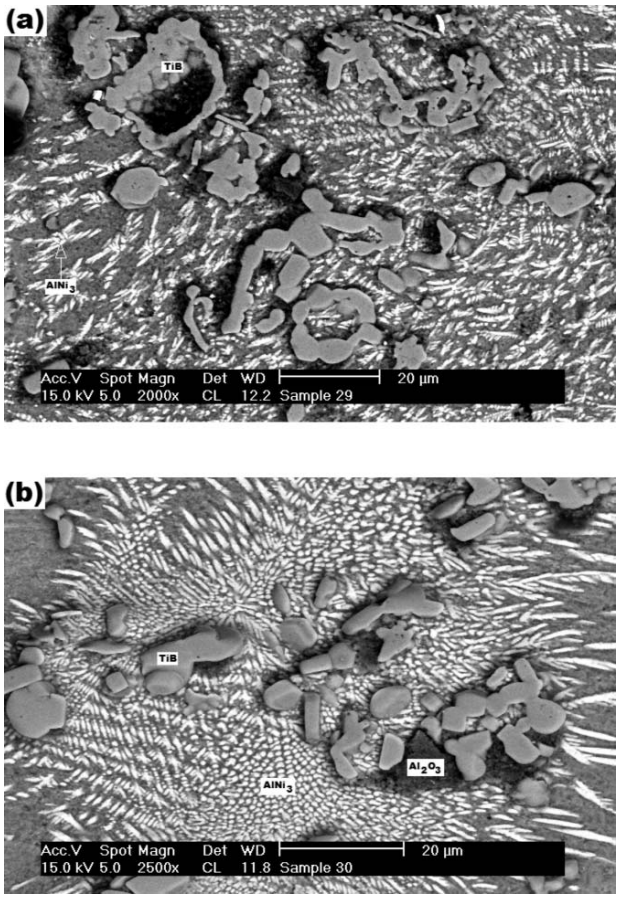

Figure 11—SEM micrographs of aluminium surface alloyed with 40% TiB_2 + 60% Ni (a) sample 29 and (b) sample 30; TiB_2, TiB phases (grey lumps; $AlNi_3$ white dendritic structure; Ni_4B_3, Al_2O_3

Table IV

Microhardness results for laser coatings

Sample no.	System (Al-TiB_2-Ni) composition	Average hardness ($HV_{0.1}$)	Depth of alloyed layer (mm)	Scan speed (m/min)
17	30%TiB_2 + 70%Ni	249	1.44	0.6
18	30%TiB_2 + 70%Ni	136	1.43	0.8
19	30%TiB_2 + 70%Ni	188	1.39	1.0
20	30%TiB_2 + 70%Ni	246	1.29	1.2
23	50%TiB_2 +50% Ni	82	1.20	0.6
24	50%TiB_2 +50% Ni	181	1.18	0.8
25	50%TiB_2 +50% Ni	184	1.16	1.0
26	50%TiB_2 +50% Ni	105	1.11	1.2
27	40%TiB_2 +60% Ni	168	1.35	0.6
28	40%TiB_2 +60% Ni	140	1.20	0.8
29	40%TiB_2 +60% Ni	154	1.11	1.0
30	40%TiB_2 +60% Ni	203	1.10	1.2

Table V

Summary of results

Sample no.	System (Al-TiB_2-Ni) composition	Average hardness (HV)
Pure Al	Al	24
100% Ni	Al-Ni	647
100% TiB_2	Al-TiB_2	58
17	30%TiB_2 + 70%Ni	249
20	30%TiB_2 + 70%Ni	246
30	40%TiB_2 + 60%Ni	203
19	30%TiB_2 + 70%Ni	188
25	50%TiB_2 + 50%Ni	184

Laser surface alloying of aluminium AA1200 with Ni and TiB_2 powders resulted in microhardness increase from 24.0 ± 0.4 HV for AA1200 to approximately 249.0 ± 0.2 HV maximum values attained for the intermetallic matrix composites fabricated. The increase in hardness of the laser-alloyed specimens was due to the presence of intermetallic compounds and solid solution hardened microstructure. The melted Ni and hard undecomposed particles significantly increased the hardness of the alloyed layer due to solution hardening, in addition to hardening arising from grain refinement.

Table V shows the summary of the results obtained for samples. From this Table, the microhardness of each of the binary system Al-Ni and Al-TiB_2 is displayed. These values can then be compared with the microhardness values for the intermetallic matrix composites. It can be seen that if only the hardness property is considered, then the Ni is very useful as reinforcement powder alone and not in combined form as MMC and intermetallics. It can be seen that sample 17 has the highest value of average microhardness out of all intermetallic matrix composites. This is closely followed by sample 20, and this improvement in hardness may be attributed to the uniform dispersion of powder obtained and also to the formation of the $AlNi_3$ intermetallics phase/dendritic microstructure evolved and the Ni_4B_3.

This improvement in hardness is over 10 times the hardness of substrate. The optimum laser processing parameters for the highest hardness is laser power 4 kW, scan speed 6.0 m/min and powder feed rate 2 rpm. The alloying powder composition for both of these samples is the same, which is 30 per cent TiB_2 + 70 per cent Ni.

Results obtained for sample 30 also showed a significant increase in microhardness, over 8 times the microhardness value of the substrate. this sample showed Ni_3B and Al_2O_3 phases. The powder mixture for this sample is 40 per cent TiB_2 + 60 per cent Ni.

Sample 19 with the powder mixture (30 per cent TiB_2 + 70 per cent Ni) also shows good microhardness. Conclusions can be made in this regard, that the 30 per cent TiB_2 + 70 percent Ni powder mixture gave the overall best microhardness properties for all intermetallic matrix composite coatings produced. It also follows that the lesser the weight per centage of TiB_2 the better the microhardness property. The presence of TiB_2 reduced the excessive hardness and brittleness of the Al-Ni dendrites.

The last sample with good microhardness property is sample 25 with the powder mixture 50 per cent TiB_2 + 50 per cent Ni. From the XRD spectrum of this sample, Ni, Ti, TiB and titanium oxide can be seen. The formation of intermetallics is much reduced here; a balance was observed between the borides and dendrites.

The microhardness/depth profile of the samples can be divided into three regions: (a) the alloyed zone, (b) the heat affected zone (HAZ) and (c) the substrate. Typically, these

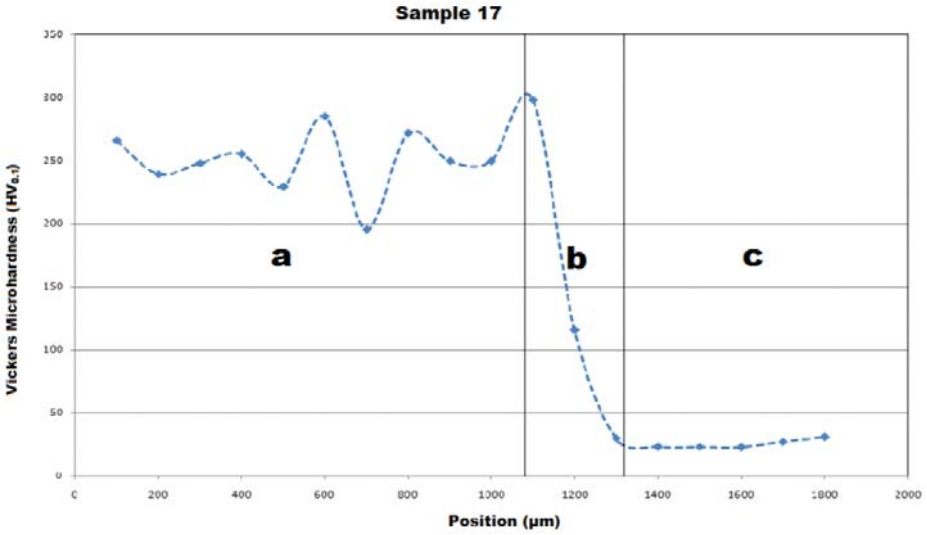

Figure 12—The microhardness/depth profile for sample 17

three regions can be seen in Figure 12 which shows the microhardness profile of sample 17. The microstructure of the alloyed zones has been discussed previously. The heat affected zone consists basically of Al in its microstructure, (see Figure 13). However, the upper portion of this zone has some sprinkles of dendrites and lumps of TiB/TiB_2. Consequently this zone is characterized by a sharp decrease in microhardness; the lower portion of the HAZ consist of Al predominantly.

Generally, it can be seen that the microhardness values of the laser coatings have significant improvement compared with the AA1200 substrate which is 24.0 ± 0.4 $HV_{0.1}$. According to the EDS analysis results, large quantities of reinforcement elements, such as Ni, Ti and B were dissolved into the matrix, which results in solution strengthening and enhances the microhardness of the matrix. In addition, the high energy density of the laser beam caused refined grain sizes.

The trend observed from the results is that the higher the percentage composition of nickel powder in the mixture, the higher the formation of the intermetallics/dendritic structure and hence the microhardness value of the alloy formed. This factor alone, however, cannot be used to draw conclusions because the microstructure formed depends largely on the laser processing parameters used. It was confirmed that the amount of the intermetallic dendritic hard phase in the laser coatings changes tremendously with increase/decrease in the composition of powder. High weight per centage of TiB_2 content is not beneficial for obtaining high hardness.

From Figure 14, no relationship can be seen between the microhardness values obtained for all samples and the scan speed. However, it was observed that the scan speed varies with depth of alloyed layer. The lower the scan speed, the bigger the depth of alloyed layer. This can be attributed to the temperature of the melt pool. The heat input is inversely proportional to the scan speed, hence the lower the scan speed the wider the melt pool. Consequently, the volume fraction of powder deposited by the lasers will also be high.

Conclusions

Different weight proportions of Ni and TiB_2 reinforcement powders were successfully laser alloyed on AA1200. The intermetallic matrix composites formed were free from cracks and pores with homogeneous dispersion of powder. The study showed that laser surface alloying led to a significant hardening effect. The microhardness of the alloyed zone was over 10 times the value of the Al-substrate. Other deductions from the study are as follows:

- The alloyed surfaces are composed of the initial phase of Al-Ni dendrites and eutectics of TiB_2/Al and TiB_2/Ni distribution on the initial phases.
- The alloyed zones consist of $AlNi_3$, Ni_4B_3 and in some coatings $TiO_{0.997}$ and Al_2O_3 dominated the alloyed zone. The heat affected zone had predominantly the initial phases which are the Al with traces of Al-Ni (dendrites) and lumps of TiB/TiB_2.
- Laser alloying with 100% Ni resulted into very high hardness values; the intermetallic dendritic phase is brittle; but laser alloying with 100% TiB_2 resulted into the formation of metal matrix composite (MMC) with relatively low hardness values. Ni is more beneficial in increasing the hardness property than the combination of MMC and intermetallic phases, if hardness is the property sought.
- The 30 per cent TiB_2 + 70 per cent Ni powder mixture gave the overall best microhardness properties out of the intermetallic matrix composites fabricated. It can be inferred that the lesser the weight per centage of TiB_2 the better the microhardness property. The presence of TiB_2 reduced the excessive brittleness of the Al-Ni dendrites; therefore brittleness of the laser alloyed surfaces can be controlled by increasing the weight proportion of TiB_2.

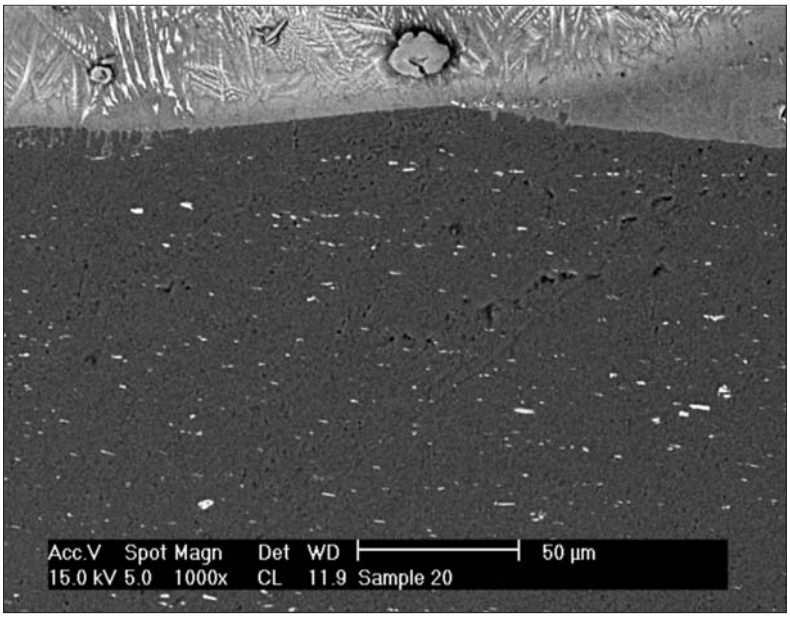

Figure 13—SEM micrograph of the heat affected zone of sample 37

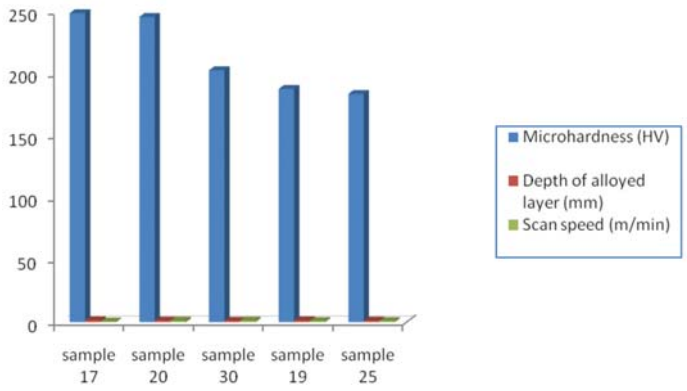

Figure 14—Variation of microhardness with scan speed and depth of alloyed layer

Acknowledgements

The author would like to thank Tshwane University of Technology and CSIR- National Laser Centre for financial support of this work.

References

Wang, X., Zhang, M., Zou, Z., and Qu, S. Microstructure and Properties of Laser Clad TiC + NiCrBSi + Rare Earth Composite Coatings. *Surface and Coatings Technology*, vol. 161, 2002. pp. 195–199.

Majumdar, J.D., Chandra, B.R., Nath, A.K., and Manna, I. *In Situ* Dispersion of Titanium Boride on Aluminium by Laser Composite Surfacing for Improved Wear Resistance. *Surface and Coatings Technology*, vol. 201, 2006. pp. 1236–1242.

Vaziri, S.R., Shahverdi, H.R., Torkamany, M.J., and Shabestari, S.G. Effect of Laser Parameters on Properties of Surface-Alloyed Al Substrate with Ni. *Optics and Lasers in Engineering*, vol. 47, 2009. pp. 971–975.

Chen, Y. and Wang, H.M. Microstructure and Wear Resistance of a Laser Clad TiC Reinforced Nickel Aluminide Matrix Composite Coating. *Materials Science and Engineering A368*, 2004. pp. 80–87.

Pardo, A., Merino, M.C., Merino, S., Viejo, F., Carboneras, M., and Arrabal, R. Influence of Reinforcement Proportion and Matrix composition on Pitting Corrosion Behaviour of Cast Aluminium Matrix Composites (A3xx.x/SiCp). *Corrosion Science*, vol. 47, 2005, pp. 1750–1764.

Chen, Y. and Wang, H.M. Microstructure of Laser Clad TiC/NiAl-Ni_3(Al,Ti,C) Wear-Resistant Intermetallic Matrix Composite Coatings. *Materials Letters*, vol. 57, 2003, pp. 2029–2036.

Pei, Y.T. and Zuo, T.C. Gradient Microstructure in Laser Clad TiC-Reinforced Ni-Alloy Composite Coating. *Materials Science and Engineering* A241, 1998, pp. 259–263.

Jiang, W.H. and Kovacevic, R. Laser Deposited TiC/H13 Tool Steel Composite Coatings and Erosion Resistance. *Journal of Materials Processing Technology*, vol. 186, 2007, pp. 331–338.

Lu, L., Lai, M.O., Su, Y., Teo, H.L., and Feng, C.F. *In situ* TiB_2 Reinforced Al Alloy Composites. *Scripta Materialia*, vol. 45, 2001, pp. 1017–1023.

Chen, Y. and Wang, H.M. Microstructure and Wear Resistance of a Laser Clad TiC Reinforced Nickel Aluminide Matrix Composite Coating. *Materials Science and Engineering* A368, 2004, pp. 80–87. ◆